

# RSC Advances



This is an *Accepted Manuscript*, which has been through the Royal Society of Chemistry peer review process and has been accepted for publication.

*Accepted Manuscripts* are published online shortly after acceptance, before technical editing, formatting and proof reading. Using this free service, authors can make their results available to the community, in citable form, before we publish the edited article. This *Accepted Manuscript* will be replaced by the edited, formatted and paginated article as soon as this is available.

You can find more information about *Accepted Manuscripts* in the [Information for Authors](#).

Please note that technical editing may introduce minor changes to the text and/or graphics, which may alter content. The journal's standard [Terms & Conditions](#) and the [Ethical guidelines](#) still apply. In no event shall the Royal Society of Chemistry be held responsible for any errors or omissions in this *Accepted Manuscript* or any consequences arising from the use of any information it contains.

## PAPER

# Fabricating Millimeter-scale Polymeric Structures for Biomedical Applications via a Combination of UV-activated Materials and Daily-use Tools

Cite this: DOI: 10.1039/x0xx00000x

Received 00th January 2012,  
Accepted 00th January 2012

DOI: 10.1039/x0xx00000x

[www.rsc.org/](http://www.rsc.org/)

Chung-Yao Yang, Chen-Meng Kuan, J. Andrew Yeh and Chao-Min Cheng\*

This paper describes an easy-to-handle approach to create three-dimensional millimeter-scale (or submillimeter-scale) polymeric structures on various substrates that have been used as molds in order to develop a polymeric-based manufacturing procedure for making *in-vitro* diagnostic devices with mass production capacity and portability. These polymeric structures were made by using UV-activated materials, adhesive tapes as the mask, and a UV-LED flashlight as the portable light source. This straightforward approach can be easily performed and has a great potential for use in resource-limited settings. The ability to conduct three common metabolic assays – for glucose, total cholesterol, and nitrite ions in this study – in both a buffer system and human serum (analytical validation, US FDA regulations) with clinically relevant sensitivity has been demonstrated using these polymeric-based *in-vitro* diagnostic devices. This study, we believe, would provide for a wide range of potential applications such as the development of *in-vitro* diagnostic devices, and a large-scale, low-cost, and easy-to-handle fabrication procedure for either developing regions or resource-limited settings, and, ultimately, for the development of “zero-cost” diagnostic devices for global public health.

## Introduction

According to the World Health Organization, *in-vitro* diagnostic devices (IVDs) for use in less economically developed regions should be “ASSURED” (affordable, sensitive, specific, user-friendly, rapid and robust, equipment-free and deliverable to end-users).<sup>1,2</sup> To date, various types of IVDs with the potential for being commercial products such as polydimethylsiloxane (PDMS)-based microfluidics, electrochemical-based glucose meters, and nitrocellulose-based lateral flow immunoassays have been extensively developed and applied in different clinically relevant situations, such as diagnosis of chronic diseases for the elderly and diagnosis of pediatric diseases for children.<sup>3-5</sup> Nowadays, there are many inexpensive commercialized lateral flow immunoassays. However, the entire cost structure for these IVDs has been significantly determined by 1) the relatively complicated fabrication procedure, e.g., SU-8 photolithography for PDMS-based microfluidics, and 2) the cost of equipment and materials, e.g., the UV exposure system or the nitrocellulose membrane for lateral flow immunoassays (~ \$10/piece).<sup>6-9</sup> Our goal is to build zero-cost *in-vitro* diagnostic devices based on current approaches. We hope to make progress toward achieving this

goal by using chemical-/physical-/engineering-based approaches to detect specific diseases (e.g., diabetes, high cholesterol level, etc.) in resource-limited and even home environments.

We, and others, have attempted to build low-cost IVDs using 1) paper as the substrate for biochemically based reactions such as enzymatic reactions (e.g., glucose oxidase or horseradish peroxidase)<sup>10-12</sup> or antibody-antigen recognitions [e.g., enzyme-linked immunosorbent assays (ELISA)],<sup>13-17</sup> and 2) a commercial wax or a laser printer as the manufacturing tool for the preparation of paper-based IVDs.<sup>18</sup> We have demonstrated the first step in the development of paper-based ELISA, which is a new and inexpensive platform that has been successfully used to create paper-based 96-well plates made using Whatman Chromatography Paper No. 1 and an SU-8 photolithography approach, for “wet-lab” biochemical analysis. We have shown that such paper-based ELISA can be used to quantify HIV-1 envelope antigen gp41 in human serum.<sup>13</sup> However, for end-users or resource-limited settings, it is still challenging to make paper-based assays using photolithography process, computer layouts, or wax printers.

Our goal is to manufacture easy-to-handle IVDs for non-technical end-users or resource-limited settings. To that end, we

continue expanding upon our previous studies to develop a “one-step process” for making three-dimensional polymeric structures at the millimeter scale in this study, which combines 1) the activation of UV-activated liquid-state materials to a solid state via a UV-LED flashlight and 2) the preparation of “masks” with the desired patterns on non-transparent adhesive tapes—in order to eliminate UV excitation in some patterned areas—using either a manual puncher or a pair of scissors. Combining all past experiences, we have developed an easy-to-handle approach to make inexpensive but robust polymeric structures with various sizes and geometries for molds, that have been used to prepare the polymeric-based platform for biochemical-based detections through the incorporation of a PDMS-based molding process with the characteristics of 1) robustness and ease of use, 2) inexpensiveness, and 3) potential expandability to mass production. This easy-to-handle approach has been demonstrated using both transparent (i.e., glass coverslip, polystyrene, polyethylene terephthalate) and non-transparent (i.e., silicon wafer, aluminum plate, iron plate, steel plate) materials as the substrate, thus demonstrating suitability of a wide array of potentially applicable substrate materials. This one-step process is also easy to operate for people who lack specific skill training, such as end-users. We have further performed three common metabolic assays—for the detections of glucose, total cholesterol, or nitrite ion ( $\text{NO}_2^-$ ) in both a buffer system and human serum—with clinically relevant sensitivity via this polymeric-based platform (i.e., PDMS-based structures), indicating that the analytical validation of this polymeric-based platform, i.e., detecting both purified glucose and cholesterol diluted in human serum, without using clinical samples from patients such as whole blood or human serum, has been achieved in this study in terms of US FDA regulations.<sup>19</sup> Not only have we successfully demonstrated these common metabolic assays but we also have developed a procedure to make PDMS-based microfluidics (see ESI), showing fabrication flexibility (for biomedically relevant applications) of this physically based approach. The development of a rapid prototyping approach in this study, we believe, would provide for a wide range of potential applications such as the development of *in-vitro* medical devices, the demonstration of easy-to-handle fabrication methods using low-cost polymers for developing or developed nations, and the development of mass production procedures.

## Experimental

### Demonstration of our easy-to-handle approach

The non-transparent adhesive tape (BT502; 50- $\mu\text{m}$ -thick backing layer and 50  $\mu\text{m}$ -thick adhesive layer) that we used as the “mask” was purchased from 3M (3M Ltd., St. Paul, MN, USA), and was patterned manually using either a manual puncher or a pair of scissors. The liquid-state UV-activated material (either OBM-309 from Orgchem Technologies Ltd., Taiwan or SU-8 2005 from MicroChem Corp., MA, USA) was dropped on the patterned regions of adhesive tape ( $\sim 3 \mu\text{L}$  for

each well), which was stuck onto the substrate. We then placed the entire setup – the liquid-state UV-activated material on the patterned adhesive tape, which was stuck onto the substrate – onto a 3 watt UV-LED flashlight as the portable UV exposure system (cost of  $\sim 60$  dollars, 400 nm, Koodyz Technology Co., Ltd., Taiwan) for 30 minutes, in order to activate the liquid-state UV-activated material (Fig. 1).

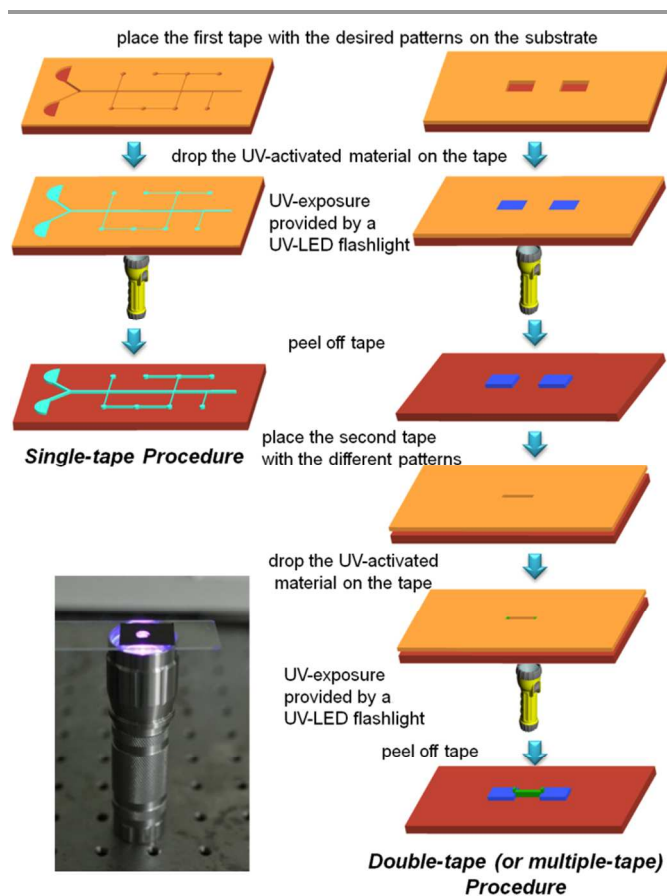


**Fig. 1** Schematic of our easy-to-handle approach using a UV-LED flashlight and adhesive tape/tape layers. The first tape with desired patterns was adhered onto the substrate and then UV-activated materials were dropped on the tape. After exposure using a UV LED flashlight for 30 minutes, the adhesive tape was peeled off to eliminate unexposed UV-activated materials and form the patterns (single-tape procedure). The different UV-activated materials can also be stacked layer by layer to form three-dimensional polymeric structures using this approach (multiple-tape procedure). The insert photography (lower left) displays the experimental setup including a UV-LED flashlight.

After the liquid-state UV-activated material—UV exposure provided by an UV-LED flashlight for a period of time (about 30 minutes for single-layer adhesive tapes)—changed its state from a liquid state to a solid state, the adhesive tape stuck onto the substrate was peeled away (i.e., lift-off process), in order to reveal the designed millimeter-scale polymeric structures with various sizes and geometries. This was completed on different low-cost substrates to create a mold for the following PDMS-based molding process.<sup>20</sup> We could also fabricate higher (thicker/taller) polymeric structures by sticking double-layer (or multiple-layer) adhesive tapes on the substrate and then dropping the UV-activated material upon our fabricated device

before UV-exposure. After the UV-activated material was activated, higher polymeric structures would be obtained (approximate time was about 45 minutes for double-layer adhesive tape structures). The height of polymeric structures was mainly determined by the number of adhesive tape layers applied to the substrate, but was affected by duration of UV exposure as well.

## Result and discussion

### Engineering performance and quality control of our easy-to-handle approach

Fig. 2a displays the adhesive tape with various complicated patterns stuck onto the glass coverslip before UV exposure. After both UV exposure and adhesive tape removal, the desired patterns were completely transferred onto the glass coverslip, as shown in Fig. 2b. We also sought to obtain a better understanding of manufacturing-based factors for our easy-to-handle approach, potentially advancing our approach an additional step from research laboratory to industrial application. In regards to this step toward real-world application, we found the following: 1) the reproducibility of simple patterns (i.e., circular or linear pattern) was better than the reproducibility of relatively complicated patterns (i.e., the edge of maple leaves) due to the potential damage resulting from peeling the adhesive tape away from the substrate (i.e., final structures with few artifacts; as arrows indicate in Fig. 2b); and, 2) the height at the edge of final polymeric structures was higher ( $\sim 5 \mu\text{m}$ ) in the central area when using OBM-309, but interestingly lower ( $\sim 6 \mu\text{m}$ ) than in the central area when we used SU-8. The results might be attributable to the coupling effects of surface tension for UV-activated materials (25.4 mN/m for OBM-309 and 33 mN/m for SU-8), and wettability of adhesive tapes and substrates. Most molecular liquids achieve complete wetting with high-energy surfaces, however, depending on the type of liquid chosen, low-energy surfaces can permit either complete or partial wetting. In addition, the contact angle of OBM-309 is lower than SU-8 2005 on the adhesive layer of the tape (see Table S1). This result could mean that OBM-309 more easily flows through the spacing between the adhesive tape and the substrate than SU-8 2005 does, therefore, the structural thickness of OBM-309 is lower than SU-8 2005 at the same volume.

Furthermore, we have made different patterns with different geometries and sizes at the millimeter scale—appropriate for the development of *in-vitro* millimeter-scale diagnostic devices while we attempt to use our naked eyes to examine diagnostic results—on various low-cost flat substrates such as polystyrene (petri dish), polyester film, glass coverslip, and silicon wafer using easy-to-handle approach, as shown in Fig. 2c-f. This indicates the versatility and substrate material of our approach. These polymeric structures adhere well onto various kinds of surfaces, and can be molded at least 100 times for PDMS molding processes. We also have attempted to make millimeter-level polymeric structures on low-cost curved

substrate using such surfaces as material from polyester spoons and glass bottles, which are commonly found in daily life, as shown in Figs. 2g and h. This procedure can help us to fabricate structures on flexible substrates, for example, we can make structures (i.e., test zones or channels) on spherical surfaces and combine PDMS molding processes to create a hollow PDMS with internal channels for biomedical applications.

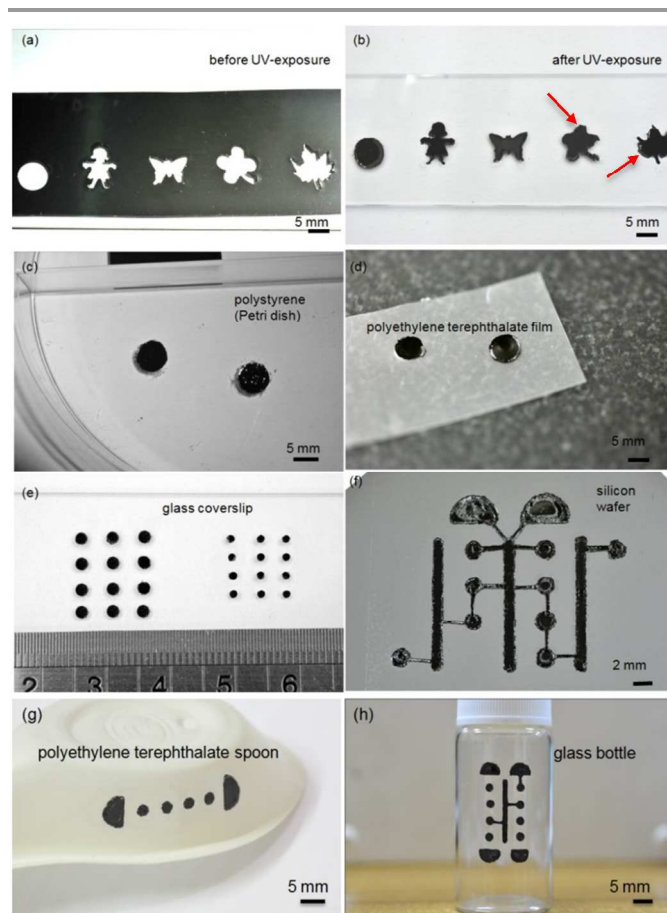


**Fig. 2** Images of polymeric structures with various patterns and sizes on different solid substrates and curved surfaces. (a) The adhesive tape with the desired geometries was made via a manual puncher. (b) The adhesive tape was peeled off after UV-LED exposure. However, there were few artifacts of final structures, as arrows indicated. The small-scale polymeric structures were fabricated via our easy-to-handle approach on various substrates: (c) Petri dish, (d) polyethylene terephthalate film, (e) glass coverslip, (f) silicon wafer, and curved surfaces: (g) polyethylene terephthalate spoon, and (h) glass bottle.

When we placed the same amount of the liquid-state UV-activated material into the same patterns on different flat substrates (polyester film, glass coverslip, and silicon wafer) in order to prepare polymeric structures using our approach, we found that the final structural heights of the polymeric structures on these flat substrates were different; the height of polymeric structures on the polyester film was about two times lower than on both the glass coverslip and silicon wafer due to different surface energies of these flat substrates, as shown in Fig. S1.

Despite the procedure of simply using single-layer adhesive tapes to make polymeric structures, we have extensively

developed different procedures, based on our easy-to-handle approach, to make three-dimensional millimeter-scale polymeric structures; for example, we have used multiple-layer adhesive tapes to create the patterns that we wanted once the polymeric structures (using just single-layer adhesive tapes) were fabricated while preparing three-dimensional polymeric structures, as shown in Fig. S2 (i.e., 10-layer structures). This

approach also has the potential to fabricate lenses with various curvatures for optical application by leveraging the different surface energies of different substrate surfaces. In addition, we could stack multiple-layer adhesive tapes to fabricate microvascular networks (e.g., animal blood vasculature and plant leaf venation) to deliver fluid or soluble product using UV-activated biomaterial microchannels.

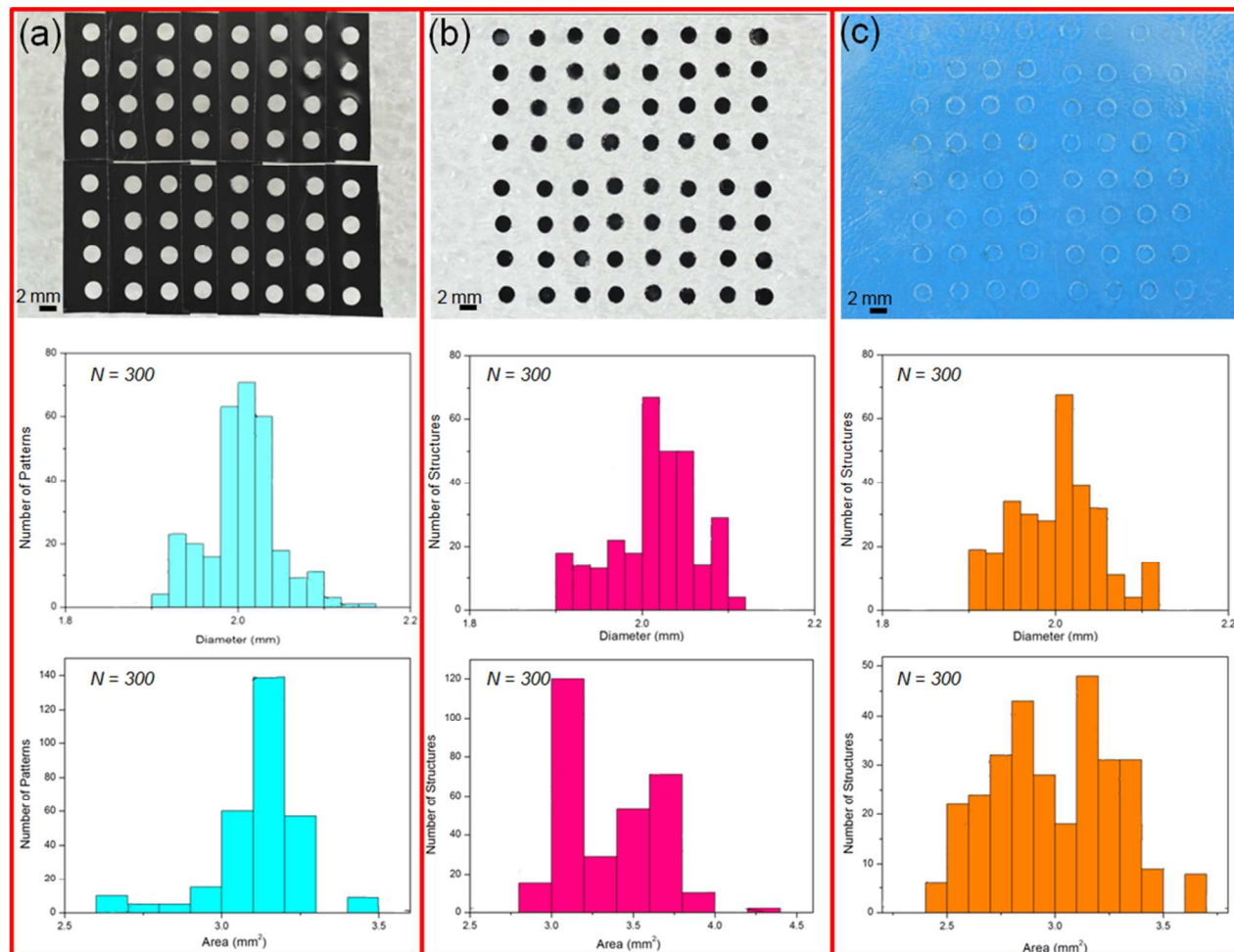


**Fig. 3** (a) Adhesive tapes with desired patterns made via a puncher with an array of 64 circular spots nominally 2 mm in diameter in upper image. The middle image is a histogram of the measured diameter for 300 circular spots shown in upper image. For the number of adhesive tapes made via a puncher in the processed image, the mean diameter was  $1.99 \pm 0.12$  mm (average  $\pm$  standard deviation,  $N = 300$ ). The lower image is a histogram of the measured area for 300 circular spots, the mean area was  $3.12 \pm 0.15$  mm<sup>2</sup> (average  $\pm$  standard deviation,  $N = 300$ ). (b) The polymeric structures with an array of 64 circular spots nominally 2 mm in diameter in upper image. The middle image is a histogram of the measured diameter for 300 polymeric structures. For the number of polymeric structures in the processed image, the mean diameter was  $2 \pm 0.1$  mm (average  $\pm$  standard deviation,  $N = 300$ ). The lower image is a histogram of measured area for 300 polymeric structures, the mean area was  $3.34 \pm 0.29$  mm<sup>2</sup> (average  $\pm$  standard deviation,  $N = 300$ ). (c) The PDMS-based structures after molding process with an array of 64 circular spots nominally 2 mm in diameter in upper image. The middle image is a histogram of the measured diameter for 300 PDMS-based structures. For the number of PDMS structures in the processed image, the mean diameter was  $1.99 \pm 0.1$  mm (average  $\pm$  standard deviation,  $N = 300$ ). The lower image is a histogram of measured area for 300 PDMS-based structures, the measured mean area of PDMS-based structures was  $2.98 \pm 0.28$  mm<sup>2</sup> (average  $\pm$  standard deviation,  $N = 300$ ).

We evaluated the performance of 1) the patterns on the adhesive tape that we prepared, 2) the exposed polymeric structures and 3) PDMS-based structures that we obtained using a PDMS-based molding process. Statistical analysis was used to provide a more comprehensive understanding of the size distribution of both patterns and structures that we obtained at different manufacturing stages (i.e., the pattern-to-pattern variation or the structure-to-structure variation). We first

prepared 300 circular patterns with a diameter of 2 mm on different adhesive tapes; Fig. 3a only shows the 64 patterns of the 300 total patterns that have been statistically analyzed. Results indicate that the measured mean diameter of these patterns was  $1.99 \pm 0.12$  mm (average  $\pm$  standard deviation,  $N = 300$ ); a histogram depicting the distribution of measured diameters). The measured mean area of these patterns has also been analyzed and found to be  $3.12 \pm 0.15$  mm<sup>2</sup> (average  $\pm$

standard deviation,  $N = 300$ ; a histogram depicting the distribution of measured areas), indicating that the area variation in this stage was about 5%. The measured mean diameter of polymeric structures (posts; Fig. 3b) was  $2 \pm 0.1$  mm (average  $\pm$  standard deviation,  $N = 300$ ), indicating that, although we used an inexpensive UV-LED flashlight to activate the liquid-state UV-activated material at this manufacturing stage in our approach, the diameter variation between structures was within the reasonable range (only 5%).

This was very challenging to achieve in terms of the quality control of large-scale manufacturing, due to the phase transition of the UV-activated material from a liquid state to a solid state. The measured mean area of polymeric structures was  $3.34 \pm 0.29$  mm<sup>2</sup> (average  $\pm$  standard deviation,  $N = 300$ ), showing an area variation of  $\sim 9\%$ , potentially resulting from the edge damages of polymeric structures while peeling off adhesive tapes. Using the PDMS-based molding process, the measured mean diameter of PDMS-based structures (wells) was  $1.99 \pm 0.10$  mm (average  $\pm$  standard deviation,  $N = 300$ ), and the diameter variation between PDMS-based structures was about 5% as well (Fig. 3c). The measured mean area of PDMS-based structures was  $2.98 \pm 0.28$  mm<sup>2</sup> (average  $\pm$  standard deviation,  $N = 300$ ) and the area variation between PDMS-based structures was about 9%. Diameter distributions of adhesive tapes, polymeric structures and PDMS-based structures are all around 2 mm. In addition, both diameter and area variations at different manufacturing stages of our approach were all within the reasonable range (all below 10%), indicating that the manufacturing reliability of our easy-to-handle approach could be used even though we attempted to make PDMS-based structures using low-cost daily-use tools and materials in this study.

In this study, we demonstrated the possibility and an idea for fabricating polymeric structures though using UV-activated materials and daily-use tools. For demonstration, we chose commonly used UV-activated materials (e.g., photoresists) and operated under atmospheric environment without handling in a fume hood and specifically protecting from light. Most of the UV-activated materials can be operated and maintained liquid state under normal condition (i.e., white light) within 20  $\sim$  30 minutes. However, the UV-activated materials used in semiconductor industry are usually eco-unfriendly. In our demonstration, though we operated the experiment outside the cleanroom, we still needed some protective equipment (i.e., anti-UV goggles and hazardous waste recycling bins for residual photoresists). However, we can use eco-friendly UV-activated materials (i.e., hydroxyethylmethacrylate) to manufacture structures for making this approach more safe for public health and environment.

#### Demonstration of metabolic assays in both buffer system and human serum

Fig. 4a illustrates the use of PDMS-based *in-vitro* diagnostic devices (wells) for the diagnosis of different analytes (nitrite ions, total cholesterol, and glucose) in both buffer system and human serum (see more experimental details in supplementary

Information). Compared with the microtiter plate that we commonly use, our device offers the advantage of considerable cost savings. Cost per diagnostic test was on the order of  $< \$0.05$  per test (e.g., PDMS-based 96-well plate, Table S3) if examined based on material preparation, manufacturing, and the fact that each test zone requires only  $\sim 2$   $\mu$ L of liquid-type sample (as opposed to the 50 or 100  $\mu$ L required for microtiter plates). We also evaluated the manufacturing cost while using conventional photolithography process (i.e., the cost of preparing a mask and the UV exposure system) to fabricate polymeric structures and PDMS-based plates. Cost per diagnostic test was on the order of  $> \$0.47$  (without considering the cost to build a clean room; Table S3). These PDMS-based IVDs can also be reused if a process of cleaning test zones with ethanol is employed, but disposable options also exist. Furthermore, both the color intensity and statistical analysis of colorimetric-based metabolic assays that we demonstrated using our device can be measured and analyzed by using software that can be installed and implemented on a cellphone (i.e., telemedicine).<sup>12</sup>

We have performed the diagnoses of glucose, total cholesterol, and nitrite ions with a lowest concentration of 1 mM, 100 mg/dL, and 0.005 mM, respectively, all in a buffer system. Despite either the wildly variable interval between meals or the occasional consumption of meals with a substantial carbohydrate load, the glucose level in blood tends to remain within the normal range; however, after eating, blood glucose levels typically increase for a short period of time (about one hour in non-diabetics) to a temporary level of as much as 7.8 mM.<sup>21,22</sup> The International Diabetes Federation (IDF) suggests that the post-meal glucose level in blood should be less than 10 mM.<sup>22,23</sup> Moreover, hypoglycemia will occur while the blood glucose levels are abnormally low, usually less than 3.9 mM<sup>24,25</sup>—an assessment level we could easily achieve using our diagnostic device (Fig. 4a). In addition, the guidelines of the American Heart Association (AHA) suggest that the total cholesterol level in blood should be below 200 mg/dL,<sup>26-28</sup> most organizations of the world agree with the AHA guidelines, although some medical doctors also suggest that cholesterol level in blood as high as 240 mg/dL would be perfectly acceptable for some patients. Under the AHA guidelines, we think that the total cholesterol level in blood ranging between 200 and 239 mg/dL should be considered “borderline”,<sup>27</sup> and levels over 240 mg/dL should be cause for concern, as it is likely indicative of risk for heart attack or stroke.<sup>29</sup> Here, we have demonstrated a total cholesterol diagnosis concentration in the buffer system of 100 mg/dL (Fig. 4a), meaning that our device has extensive potential for use in clinically relevant applications. For total cholesterol diagnosis in the buffer system, it is clinically meaningless to diagnose total cholesterol of low concentrations, compared with either glucose diagnosis or nitrite ion analysis; for this reason, we elected to detect total cholesterol in the buffer system only in the range of 100 to 600 mg/dL (Fig. 4a).

Nitrite ions are not one of the normal components in human urine; they are, however, indicative of either urinary tract

infections or bacterial infections in terms of urine-based diagnosis. Therefore, the limit of detection of nitrite ions is as low as possible for the *in-vitro* urinary diagnostic devices. Fig. 4b-d illustrates the mean intensity of three metabolic assays (glucose, total cholesterol, and nitrite ions, all in the buffer system, respectively;  $N = 20$ ) at various concentrations

using image data analysis, ImageJ (described in Supplementary Information), indicating that mean intensity can be discriminated while performing these metabolic assays using our device, which displays a clearly excellent linear relationship at lower concentrations.

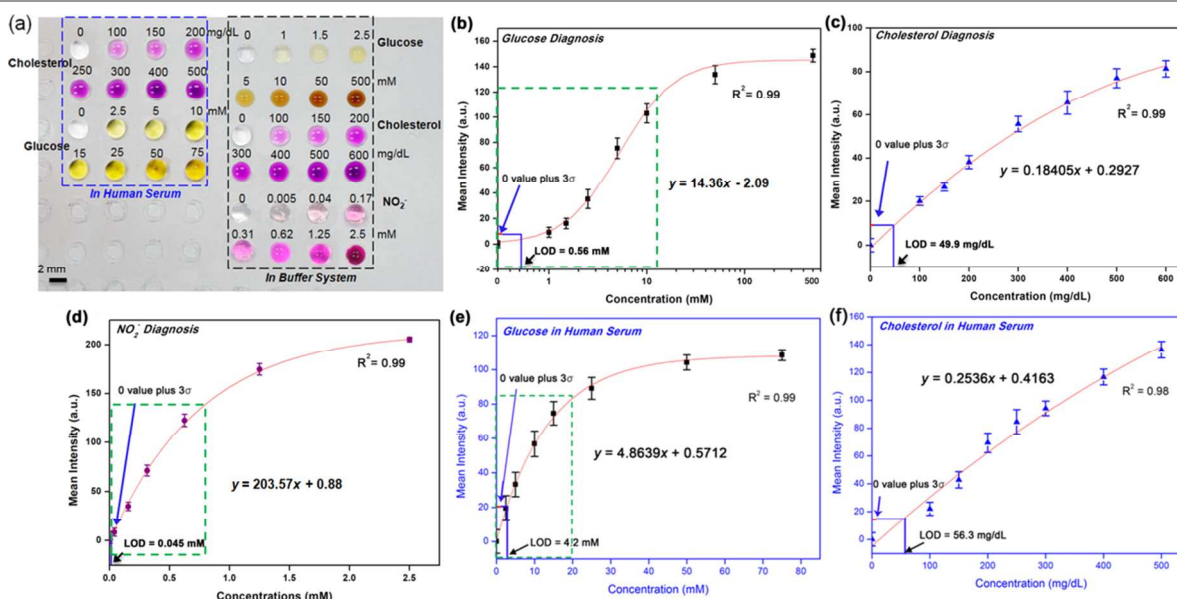


**Fig. 4** (a) Demonstration of colorimetric-based metabolic assays by remodeling the polymeric structures via PDMS-based molding process. These images were captured with a digital camera. Glucose with various concentrations in buffer system can be detected from 100 to 600 mg/dL. Nitrite ion with various concentrations in buffer system can be detected from 0.005 to 2.5 mM. Cholesterol and glucose diluted in human serum can also be detected at low concentrations from 100 mg/dL and 2.5 mM, respectively, suggesting that our diagnostic device combined with metabolic assays are suitable for clinically relevant applications. (b, c, d) Mean intensity of glucose, cholesterol and nitrite ion at various concentrations in buffer system calculated via ImageJ, respectively. Data are mean  $\pm$  standard deviation ( $N = 20$ ) for all detections. For the detections, the data showed linear relationship at low concentrations. (e, f) Mean intensity of glucose and cholesterol at various concentrations in human serum calculated via ImageJ, respectively. Data are mean  $\pm$  standard deviation ( $N = 20$ ) for all detections.

To demonstrate analytical validation of our diagnostic device for three metabolic assays, we also have performed the diagnosis of both glucose and total cholesterol levels in human serum. It is noted that we used US FDA regulations for IVD performance evaluation with the appropriate data analysis as an ideal standard. For glucose level diagnosis in human serum (Fig. 4a), the mean intensity of this diagnosis obviously increased, compared with results obtained using our buffer system (Fig. 4a), strongly suggesting that our diagnostic device (with glucose assay) was appropriate for clinical use. For total cholesterol level diagnosis in human serum (Fig. 4f), the color change from colorless to purple seen in this assay can also be obtained while performing this enzymatic reaction for 30 minutes. The limit of detection (LOD) was calculated to be the concentration that generated an intensity level three times the standard deviation of intensities measured in zero concentration AU (all calculations were conducted at linear regions). The limit of detection of glucose, cholesterol and nitrite ions in buffer system is 0.56 mM, 49.88 mg/dL, and 0.045 mM, respectively. We also compared our results (e.g., glucose, total cholesterol and nitrite ions) with point-of-care diagnostic devices.<sup>30-32</sup> Määttänen *et al.* demonstrated paper-based point-of-care diagnostic device for testing glucose at a detection limit

of 0.56 mM, which was similar to our result.<sup>30</sup> de Souza *et al.* demonstrated a toner-based microfluidics device made by polyester film for testing glucose and cholesterol with the LODs of 1.7 mM and 20 mg/dL, respectively.<sup>31</sup> Klasner *et al.* also demonstrated paper-based diagnostic device for testing nitrite in saliva with the LOD of 0.005 mM.<sup>32</sup> In our system, we can detect nitrite ions at 0.005 mM, however, it is difficult to distinguish the color intensity between blank and 0.005 mM via imaging software (LOD = 0.045 mM). The limit of detection of glucose and cholesterol in human serum system is 4.2 mM and 56.3 mg/dL, respectively. Both the detection limit and sensitivity of metabolic-based assays have been recognized as relating to the physical adsorption of liquid-type reagents onto used substrates (e.g., filter paper, nitrocellulose membrane, microtiter plate). We found that the physical absorption of liquid-type reagents onto PDMS would be relatively less than either filter paper or nitrocellulose membrane due to its hydrophobicity. This means there would be less physically based interactions between PDMS and liquid-type reagents, compared with the use of either filter paper or nitrocellulose membrane as the substrate to make IVDs. Therefore, we could obtain a stronger output color signal using PDMS than when using paper as a substrate.

## Conclusions

The process or means by which to simplify the manufacturing process for *in-vitro* diagnostic devices has long been an interesting topic for a variety of research communities including those concerned with biomedical or point-of-care applications. Such pursuits have, and continue to be, especially relevant for resource-limited areas, but are capable of providing significant cost-savings for any economy. To address this issue, we have developed an inexpensive but robust and easy-to-handle approach for fabricating polymeric structures using daily-use tools and materials, including a UV-LED flashlight, manual punchers, and adhesive tapes. Through our easy-to-handle approach, three-dimensional polymeric structures can also be fabricated via multiple-layering of adhesive tapes and offers considerable potential for the creation of “zero-cost” biomedical devices. In this study, the PDMS-based molding process can be used to fabricate PDMS-based IVDs with a manufacturing duration of less than one hour and a cost of \$0.05 per diagnostic test. The diagnosis of glucose, total cholesterol, and nitrite ion levels in a buffer system as well as in human serum has been demonstrated with clinically relevant sensitivity, illustrating the potential of our diagnostic device for clinically relevant applications.

## Acknowledgements

We would like to thank the National Science Council of Taiwan for financially supporting this research under Contract No. NSC 101-2221-E-007-113-MY3 (to J. A. Yeh), NSC 101-2628-E-007-011-MY3 (to C.-M. Cheng), NSC 101-2325-B-006-021 (to C.-M. Cheng), and the grant for Interactive Nano/MicroElectroMechanical Components and Systems from National Tsing Hua University, Taiwan (to J. A. Yeh and C.-M. Cheng).

## Notes and references

<sup>a</sup> Institute of Nanoengineering and Microsystems National Tsing Hua University. No. 101, Section 2, Kuang-Fu Road, Hsinchu 30013, Taiwan. Email: [chaomin@mx.nthu.edu.tw](mailto:chaomin@mx.nthu.edu.tw).

Electronic Supplementary Information (ESI) available: Experimental details and microfluidic demonstration. See DOI: 10.1039/b000000x/

- C. Deal, W. Cates, R. Peeling and A. Wald, *Emerg. Infect. Dis.*, 2004, **10**, e2.
- R. W. Peeling, K. K. Holmes, D. Mabey and A. Ronald, *Sex. Transm. Infect.*, 2006, **82**, v1.
- Z. Tang, J. H. Lee, R. F. Louie and G. J. Kost, *Arch. Pathol. Lab. Med.*, 2000, **124**, 1135.
- S. Wang, C. Zhang, J. Wang and Y. Zhang, *Anal. Chim. Acta.*, 2005, **546**, 161.
- A. C. Cazacu, J. Greer, M. Taherivand and G. J. Demmler, *J. Clin. Microbiol.*, 2003, **41**, 2132.
- E. Kim, Y. Xia and G. M. Whitesides, *Nature*, 1995, **376**, 581.
- D. C. Duffy, J. C. McDonald, O. J. A. Schueller and G. M. Whitesides, *Anal. Chem.*, 1998, **70**, 4974.

- J. N. Lee, C. Park and G. M. Whitesides, *Anal. Chem.*, 2003, **75**, 6544.
- K. J. Regehr, M. Domenech, J. T. Koepsel, K. C. Carver, S. J. Ellison-Zelski, W. L. Murphy, L. A. Schuler, E. T. Alarid and D. J. Beebe, *Lab Chip*, 2009, **9**, 2132.
- A. W. Martinez, S. T. Phillips, M. J. Butte and G. M. Whitesides, *Angew. Chem.*, 2007, **119**, 1340.
- A. W. Martinez, S. T. Phillips and G. M. Whitesides, *Proc. Natl. Acad. Sci. USA*, 2008, **105**, 19606.
- A. W. Martinez, S. T. Phillips, E. Carrilho, S. W. Thomas, H. Sindi and G. M. Whitesides, *Anal. Chem.*, 2008, **80**, 3699.
- C.-M. Cheng, A. W. Martinez, J. Gong, C. R. Mace, S. T. Phillips, E. Carrilho, K. A. Mirica and G. M. Whitesides, *Angew. Chem.*, 2010, **122**, 4881.
- X. Liu, C.-M. Cheng, A. W. Martinez, K. A. Mirica, X. J. Li, S. T. Phillips, M. Mascarenas and G. M. Whitesides, “A portable microfluidic paper-based device for ELISA,” in *Micro Electro Mechanical Systems (MEMS), 2011 IEEE 24th International Conference on* Cancun, 23-27 Jan., 2011, 75.
- S.-J. Lo, S.-C. Yang, D.-J. Yao, J.-H. Chen, W.-C. Tu and C.-M. Cheng, *Lab Chip*, 2013, **13**, 2686.
- H.-K. Wang, C.-H. Tsai, K.-H. Chen, C.-T. Tang, J.-S. Leou, P.-C. Li, Y.-L. Tang, H.-J. Hsieh, H.-C. Wu and C.-M. Cheng, *Adv. Healthcare Mater.*, 2014, **3**, 187.
- M.-Y. Hsu, C.-Y. Yang, W.-H. Hsu, K.-H. Lin, C.-Y. Wang, Y.-C. Shen, Y.-C. Chen, S.-F. Chau, H.-Y. Tsai and C.-M. Cheng, *Biomaterials*, 2014, **35**, 3729.
- G. V. Kaigala, S. Ho, R. Penterman and C. J. Backhouse, *Lab Chip*, 2007, **7**, 384.
- Guidance for Industry: Analytical Procedures and Methods Validation. US Food and Drug Administration, July 2000.
- Y. Xia and G. M. Whitesides, *Angew. Chem. Int. Ed.*, 1998, **37**, 550.
- M. E. Daly, C. Vale, M. Walker, A. Littlefield, K. G. Alberti and J. C. Mathers, *Am. J. Clin. Nutr.*, 1998, **67**, 1186.
- Guideline for Management of PostMeal Glucose in Diabetes. International Diabetes Federation, 2011.
- The Global IDF/ISPAD Guideline for Diabetes in Childhood and Adolescence. International Diabetes Federation, 2011.
- W. L. Clarke, D. J. Cox, L. A. Gonder-Frederick, D. Julian, D. Schlundt and W. Polonsky, *Diabetes Educator*, 1997, **23**, 55.
- The information also can be found at American Diabetes Association (ADA) website: <http://www.diabetes.org/living-with-diabetes/treatment-and-care/blood-glucose-control/hypoglycemia-low-blood.html>.
- N. J. Stone, J. Robinson, A. H. Lichtenstein, C. N. B. Merz, C. B. Blum, R. H. Eckel, A. C. Goldberg, D. Gordon, D. Levy, D. M. Lloyd-Jones, P. McBride, J. S. Schwartz, S. T. Shero, S. C. Smith, Jr. K. Watson and P. W. F. Wilson, *Circulation*, 2013. DOI: 10.1161/01.cir.0000437738.63853.7a.
- Expert Panel on Detection, Evaluation, and Treatment of High Blood Cholesterol in Adults, *JAMA*, 2001, **285**, 2486.
- The information also can be found at American Heart Association (AHA) website: [http://www.heart.org/HEARTORG/Conditions/Cholesterol/AboutCholesterol/What-Your-Cholesterol-Levels-Mean\\_UCM\\_305562\\_Article.jsp](http://www.heart.org/HEARTORG/Conditions/Cholesterol/AboutCholesterol/What-Your-Cholesterol-Levels-Mean_UCM_305562_Article.jsp)

- 29 A. Wisitsorrat, P. Sritongkham, C. Karuwan, D. Phokharatkul, T. Maturros and A. Tuantranont, *Biosens. Bioelectron.*, 2010, **26**, 1514.
- 30 A. Määttänen, D. Fors, S. Wang, D. Valtakari, P. Ihalainen and J. Peltonen, *Sens. Actuators B: Chem.*, 2011, **160**, 1404.
- 31 F. R. de Souza, G. L. Alves and W. K. T. Coltro, *Anal. Chem.*, 2012, **84**, 9002.
- 32 S. A. Klasner, A. K. Price, K. W. Hoeman, R. S. Wilson, K. J. Bell and C. T. Culbertson, *Anal. Bioanal. Chem.*, 2010, **397**, 1821.